

# MAGNETOELECTRIC RESONANT GATE TRANSISTOR

F. Li<sup>1\*</sup>, R. Misra<sup>2</sup>, Z. Fang<sup>1</sup>, C. Curwen<sup>1</sup>, Y. Wu<sup>1</sup>, Q. M. Zhang<sup>1,3</sup>, P. Schiffer<sup>2,3</sup>, S. Tadigadapa<sup>1,3</sup> and S. Datta<sup>1,3</sup>

<sup>1</sup>Electrical Engineering, <sup>2</sup>Physics Department, and <sup>3</sup>Materials Research Institute, The Pennsylvania State University, University Park, Pennsylvania 16802, USA

## ABSTRACT

Chip scale, high sensitivity magnetic sensor arrays capable of sensing below 100 picoTesla vector fields are of great interest to biomedical applications such as noninvasive medical imaging and diagnosis. Here, we present an integrated magnetolectric resonant gate transistor (ME RGT) with nanoTesla magnetic field detection sensitivity. The device integrates Titanium (Ti)-Metglas<sup>®</sup> ( $\text{Fe}_{0.85}\text{B}_{0.05}\text{Si}_{0.1}$ ) based magnetostrictive unimorph freestanding cantilever beam coupled capacitively to the gate of an n-channel field effect transistor (FET). Using this configuration at the flexural resonance frequency of 4.9 kHz of the cantilever, a signal-to-noise ratio of 646,000 $\sqrt{\text{Hz/Oe}}$  and a minimum detectable field of  $15 \times 10^{-11} \text{T}/\sqrt{\text{Hz}}$  were obtained at room temperature. This result shows a significant improvement in the thin film ME sensor integration with standard CMOS process towards on-chip biomedical imaging applications.

## INTRODUCTION

Magnetolectric (ME) effect [1] is defined as the induction of electrical polarization upon application of a magnetic field H and/or the magnetization upon application of an electric field E. Research has been done on both single phase materials [2] (e.g.  $\text{Cr}_2\text{O}_3$ ) and composite laminates (e.g. PZT/ Terfenol-D, PVDF/Metglas<sup>®</sup>) constructed out of a bi-layer of a magnetostrictive and piezoelectric materials. Unlike single phase materials, composite laminates have the advantage that each layer can be independently optimized to achieve a high effective ME coefficient. Recently, bulk sensors made by ME laminates were reported to exhibit large ME coupling coefficient of 21.46 V/cm $\cdot$ Oe [3] and a high sensitivity of  $2 \times 10^{-11} \text{T}/\sqrt{\text{Hz}}$  [4]. However, these bulk sensors suffer from several drawbacks: (i) the size of the current prototypes of 2 – 10 cm are too large for monolithic integration with CMOS circuits and chip scale sensor arrays, (ii) the strength of coupling of the magnetic field induced strain to the piezoelectric layer is typically reduced by bonding epoxy layers [5]-[7]. In this work, we present a Metglas<sup>®</sup> ( $\text{Fe}_{0.85}\text{B}_{0.05}\text{Si}_{0.1}$ ) thin film magnetolectric resonant gate transistor (MERGT) by integrating a resonant magnetostrictive (MS) cantilever sensor directly atop a sensing and amplifying transistor, as shown in Fig. 1. The magnetostrictive cantilever is made from Ti/Metglas<sup>®</sup> thin film unimorph and thus can be readily integrated with the NMOS transistor readout and avoids the use of any epoxy bonding layer.

## THIN FILM METGLAS<sup>®</sup> AND RESONANT GATE

The magnetolectric resonant gate transistor combines the benefits of high-deflection sensitivity of MS cantilever sensors and FET motion sensing. A small time varying magnetic field is sensed by the resonant gate (suspended cantilever) via magnetostrictively induced flexural bending of the cantilever which, in turn, modulates the air-gap capacitance. This in turn modulates the channel charge density and therefore produces a proportional change in the drain current of the transistor amplified by the transconductance of the FET.

In order to characterize the magnetic properties of the deposited Metglas<sup>®</sup> films, 150 nm thick films were first deposited on a silicon substrate and cut into 15 mm x 3 mm cantilevers. The magnetic hysteresis loop is measured by Quantum Design

superconducting quantum interference device (SQUID) magnetometer. The samples are loaded in a plastic straw with the plane of the film in a direction parallel to the magnetic field. The magnetic field dependence of the magnetic moment is studied at 293 K. The deposited films exhibit low coercive field and high saturation magnetization, as shown in Fig. 2.

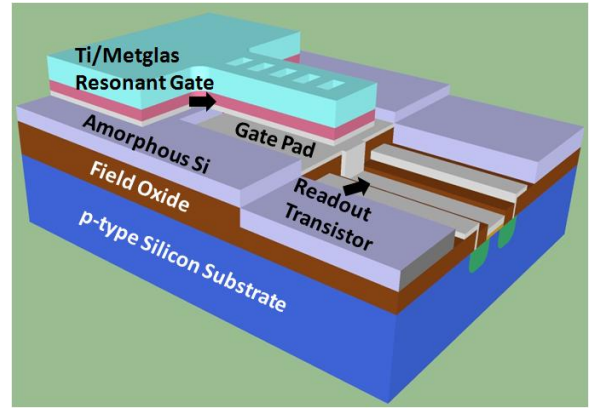


Figure 1: Schematic of the magnetolectric resonant gate transistor (MERGT).

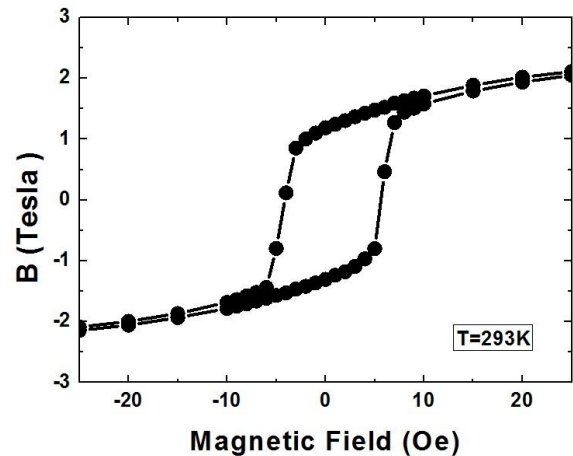


Figure 2: B-H hysteresis loop of the 150 nm thick ion-beam deposited Metglas<sup>®</sup> film.

Magnetostrictive coefficient of the films was characterized by using a laser vibrometer. The test cantilever was one end clamped onto the substrate holder. The entire sample was placed in a Helmholtz coil and the deflection of the silicon cantilever was accurately measured as a function of the applied magnetic field as shown in the inset of Fig. 3. Figure 3 shows the measured magnetostrictive coefficient as a function of the applied magnetic field. The maximum response occurs at 4 (-3) Oe.

The fabrication of the MERGT is realized on a NMOS transistor platform. Briefly, 5 m NMOS transistors with platinum gate are fabricated on p-type silicon wafers. This is followed by the

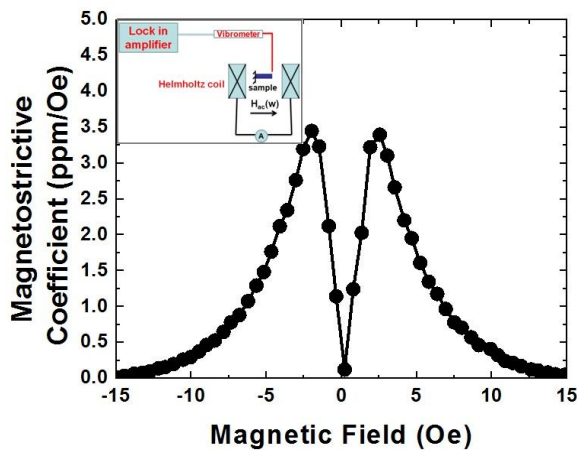


Figure 3: Magnetostrictive coefficient as a function of DC magnetic field. (Inset: laser vibrometer setup for MS coefficient characterization)

deposition of amorphous silicon sacrificial layer. The magnetostrictive cantilever consisting of 150 nm thick Metglas<sup>®</sup> film on 500 nm thick titanium films is patterned via lift-off process. Finally, the cantilevers are released using XeF<sub>2</sub> vapor phase etching of the sacrificial amorphous silicon while protecting the anchor and other transistor regions by photoresist pattern.

Further details on the fabrication process can be found in reference [8]. Figure 4 shows the ZYGO<sup>®</sup> image of the freestanding magnetostrictive cantilever forming the gate electrode of the MERGT. An inherent problem associated with the bilayer thin film MS cantilevers is the zero field curvature of the released cantilever beam due to the residual stress mismatch between films. As can be seen from the white light interferometric image of the cantilever at zero field (inset Fig. 4), the freestanding MS cantilever is bent upwards by 5 μm at the tip end due to the larger residual tensile stress in the Metglas<sup>®</sup> film in comparison to that of the Ti passive layer and therefore results in a smaller air gap capacitance.

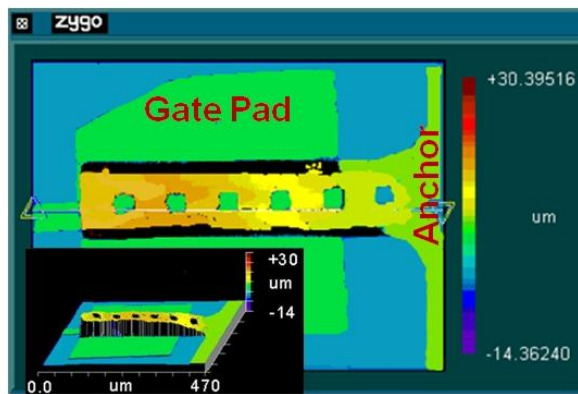


Figure 4: Top view Zygo<sup>®</sup> image (SEM) of a 300 μm long and 100 μm wide resonant gate. (Inset: 3D ZYGO<sup>®</sup> image of the magnetostrictive top resonant gate)

We used a custom designed optical set-up to verify the functionality of the top resonant gate. The experimental set-up uses a position sensitive photo detector (PSD) to measure the deflection of the beam, as illustrated schematically in Fig. 5. A 600 nm wavelength laser is focused and directed onto the resonant gate tip

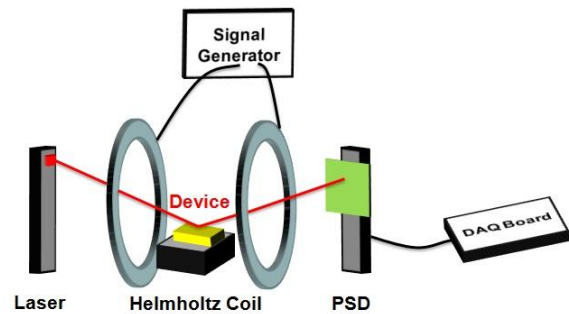


Figure 5: Schematic of optical measurement set-up using position sensitive photo detector.

and is actuated by the magnetic field generated using a Helmholtz coil. The reflected laser beam is detected by the Stiek Electro-Optics 2D PSD and the output acquired using a National Instruments<sup>®</sup> data acquisition box. HP 3314A function generator was used to drive the Helmholtz coil using a triangle wave with 95%-5% symmetry to output a 0 – 1 Oe magnetic field.

Figure 6 plots the output of PSD, which shows a linearly decreasing output as a function of the applied magnetic field using the Helmholtz coil. This result confirms that the freestanding magnetostrictive cantilever responds to the incident magnetic signal via flexural bending. Calibrating the applied magnetic field the response of the PSD can be converted into an optically measured sensitivity of 4 mV/Oe.

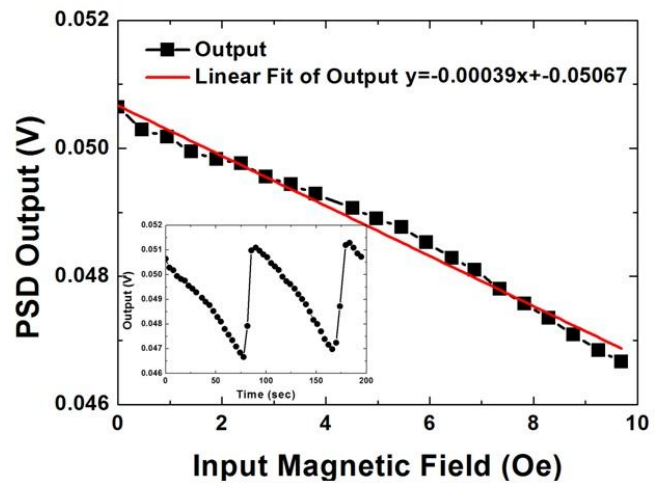
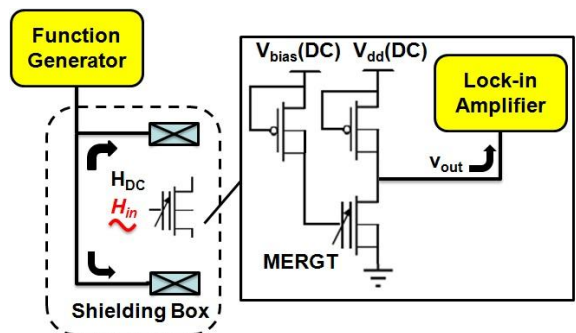


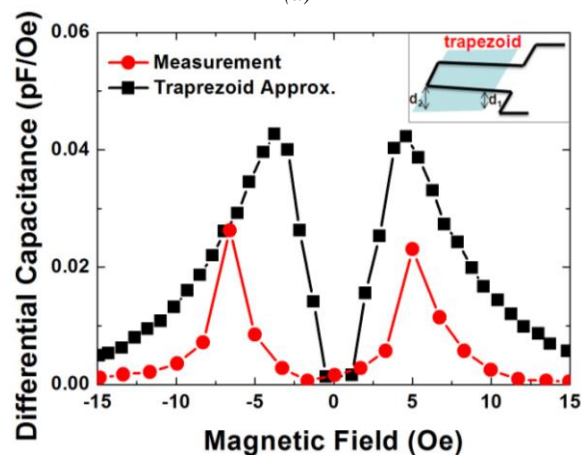
Figure 6: PSD output varies linearly with input magnetic field. (Signal generator provides a triangle wave with 95%-5% symmetry at a frequency of 0.01 Hz, 5.95 V<sub>pp</sub>, with an offset of 3.0 V.)

## MERGT CHARACTERIZATION AND DISCUSSION

For the complete electrical characterization, the devices are placed in a ceramic dual in-line package and wire bonded to make electrical connections to the device. The performance of the MERGT was then tested in the configuration as shown in Fig. 7(a). The electromagnet controlled by the function generator provides both input ac magnetic field,  $H_m$ , and the DC magnetic bias field,  $H_{DC}$ . We first characterized the top resonant gate capacitance performance. The change in capacitance was measured at 100 Hz with a DC magnetic bias field using an Andeen Hagerling ultra



(a)



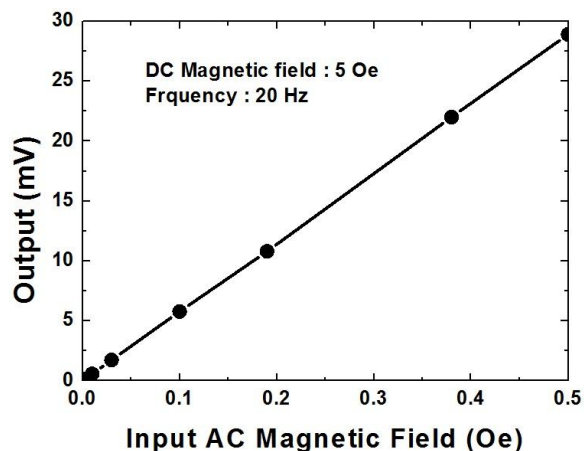
(b)

Figure 7: (a) Schematic of ac magnetic field measurement set-up. (b) Input capacitance change (measurement and calculation) as a function of DC magnetic field.

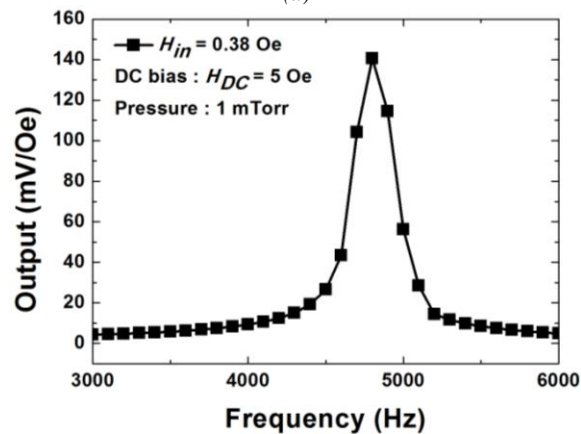
precision capacitance bridge (AH 2700A). The results, displayed in Fig. 7(b), show the comparison of differential capacitance between measurement and analytical approximation as a function of the DC magnetic bias field. The trapezoidal gap approximation for the based on a linearly bent cantilever profile overestimates the capacitance of the device and results in a shift of the peak response magnetic field. The model needs to include the 2D bowing of the cantilever structure to find a good agreement with the measured results [8]. The peak AC response happened at 5 (-6) Oe.

Figure 8 shows the characterization of a completed MERGT. The output of the FET was measured using a Stanford Research SRS-830 Lock-in Amplifier. The output voltage vs. input ac magnetic field was performed in Fig. 8 (a). The measurement shows the linearity of the common source readout amplifier output following the input magnetic signal. The DC bias magnetic field was fixed at 5 Oe where the device output shows the peak response. The frequency response of the MERGT was studied in vacuum ( $10^{-3}$  Torr), as shown in Fig. 8 (b). The device was biased for the maximum ac response by a permanent magnet and then pumped down to milli-Torr pressure range using a dry pump. After the pressure had stabilized, the chamber was valved-off to maintain the chamber pressure and the chamber was physically disconnected from the pump to isolate it from the external mechanical vibration. The ac input magnetic field was then generated by a Helmholtz coil. At resonance, the output voltage increases by  $\sim 20$  (in vacuum). The noise spectrum of MERGT is shown in Fig. 8 (c). The flicker noise of the input transistor limits the noise floor of the whole system [9]. Based on the results in Figs 8, we can obtain a

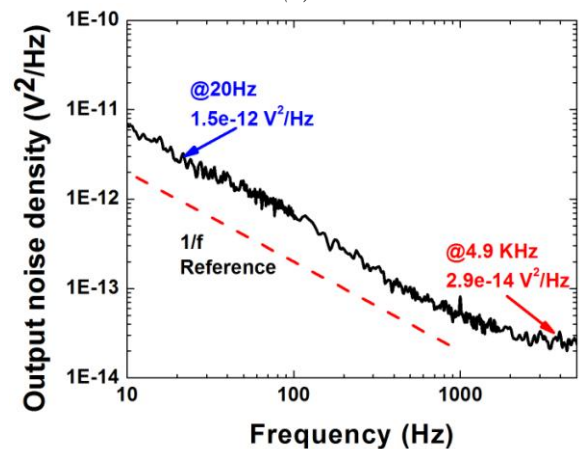
signal-to-noise ratio of  $646,000 \sqrt{\text{Hz/Oe}}$  ( $40,800 \sqrt{\text{Hz/Oe}}$ ) at (off) resonance, which corresponds to a minimum detectable field of  $150 \text{ pT}/\sqrt{\text{Hz}}$  ( $3 \text{ nT}/\sqrt{\text{Hz}}$ ). This result represents a significant enhancement in comparison to the first integrated ME sensor demonstrated by Y. Lu and A. Nathan with 40 micro Tesla detectable field [10].



(a)



(b)



(c)

Figure 8: (a) Output voltage of common source readout amplifier circuit as a function of the input ac magnetic field. The data was measured at 20 Hz and  $H_{DC} = 5$  Oe. (b) MERGT frequency response measurement in vacuum. (c) Output noise performance of MERGT.

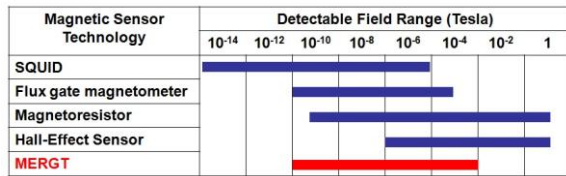


Figure 9: MERGT sensitivity in comparison with current magnetic sensing technologies.

Finally, we have benchmarked our MERGT performance [8] in Fig. 9 by comparing the results in this work to the current magnetic sensing technologies [11] with other types of magnetic field sensors. The sensitivity of MERGT is close to the flux gate magnetometer and has the potential to achieve picoTesla detection currently achievable only using SQUID sensors. It should be noted that the noise level in this work is limited by the flicker noise of sensing transistors. By using advanced transistors such as SiGe Quantum well FETs with much lower flicker noise the overall noise can be reduced by at least two orders of magnitude. Furthermore, by better controlling the stress mismatch of the two constituent layers (Ti and Metglas<sup>®</sup>), the sensitivity can be further improved. These considerations suggest a strong potential of the next generation MERGT in achieving picoTesla detection at room temperature.

## CONCLUSION

In summary, an integrated Metglas<sup>®</sup> MERGT with nanoTesla detection at resonance has been designed, fabricated and modeled. Such MEMS-NMOS integration using magnetostrictive cantilever and FET sensing and amplifying capability exhibits a significant enhancement in the signal-to-noise ratio and consequently smaller minimum detectable magnetic field. Also, this demonstration indicates the compatibility of the ME sensors integration with the Si process technology and suggests the future solutions for the ultra sensitive chip-scale magnetometers implementation.

## ACKNOWLEDGMENT

The nanofabrication of the MERGT was performed at Pennsylvania State University Nanofab supported by the National Nanotechnology Infrastructure Network (NNIN). Also, the authors gratefully acknowledge the support of Jose Israel Ramirez and Thomas Jackson from Pennsylvania State University for the Metglas<sup>®</sup> ion mill sputtering.

Travel support has been generously provided by the Transducer Research Foundation.

## REFERENCES

[1] L. D. Landau and E. M. Lifshitz, "Electrodynamics of Continuous Media" 1960, pp. 119-120.  
 [2] G. T. Rado and V. Folen, "The effective magnetoelectric coefficients of polycrystalline Cr<sub>2</sub>O<sub>3</sub> annealed in perpendicular electric and magnetic fields," J. Phys. Rev. Lett., vol. 7, pp. 310, 1961.  
 [3] Z. Fang, S. G. Lu, F. Li, S. Datta, and Q. M. Zhang, "Enhancing the Magnetoelectric Response of Metglas/Polyvinylidene fluoride Laminates by Exploiting the Flux Concentration Effect," Appl. Phys. Lett., vol. 95, 112903, 2009.

[4] J. Zhai, Z. Xing, S. Dong, J. Li, and D. Viehland, "Detection of pico-Tesla magnetic fields using magnetoelectric sensors at room temperature," Appl. Phys. Lett., vol. 88, 062510, 2006.  
 [5] S. Dong, J. Zhai, J. Li, D. Viehland, "Near-ideal magnetoelectricity in high-permeability magnetostrictive piezofibere laminates with a (2-1) connectivity," Appl. Phys. Lett., vol. 89, 252904, 2006.  
 [6] Y. Wang, D. Gray, D. Berry, J. Gao, M. Li, F. Li, and D. Viehland, "An Extremely Low Equivalent Magnetic Noise Magnetolectric Sensor," Adv. Mater., vol. 23, pp. 4111-4114, 2011.  
 [7] F. Li, F. Zhao, Q. M. Zhang and S. Datta, "Low-frequency voltage mode sensing of magnetoelectric sensor in package," Electronics Letters, vol. 46, no. 16, 2010.  
 [8] F. Li, R. Misra, Z. Fang, Y. Wu, Q. M. Zhang, P. Schiffer, S. Tadigadapa and S. Datta, "Magnetolectric Resonant Gate Transistor with NanoTesla Sensitivity," submitted to Journal of MEMs, 2012.  
 [9] F. Li, Z. Fang, R. Misra, S. Tadigadapa, Q. M. Zhang, and S. Datta, "Giant Magnetoelectric Effect in Nanofabricated Pb(Zr<sub>0.52</sub>Ti<sub>0.48</sub>)O<sub>3</sub>-Fe<sub>0.85</sub>B<sub>0.5</sub>Si<sub>0.1</sub> Cantilevers and Resonant Gate Transistors," Device Research Conference, vol. 37, no. 69, 2011.  
 [10] Y. Lu, and A. Nathan, "Thin film magnetostrictive sensor with on-chip readout and attofarad capacitance resolution," IEEE Int. Electron Devices Meet., pp. 777-780, 1996.  
 [11] M. J. Caruso, T. Bratland, C. H. Smith, R. Schneider, Honeywell, Inc.

## CONTACT

\*F. Li, Tel: +1-814-321-6158; fxl135@psu.edu